

# Optical Engineering

[SPIDigitalLibrary.org/oe](http://SPIDigitalLibrary.org/oe)

## **Fiber-optic ultrasound generator using periodic gold nanopores fabricated by a focused ion beam**

Ye Tian  
Nan Wu  
Xiaotian Zou  
Haitham Felemban  
Chengyu Cao  
Xingwei Wang

# Fiber-optic ultrasound generator using periodic gold nanopores fabricated by a focused ion beam

**Ye Tian**

**Nan Wu**

University of Massachusetts Lowell  
Department of Electrical and Computer  
Engineering  
Lowell, Massachusetts 01854

**Xiaotian Zou**

University of Massachusetts Lowell  
Department of Biomedical and Biotechnology  
Engineering  
Lowell, Massachusetts 01854

**Haitham Felemban**

**Chengyu Cao**

University of Connecticut  
Department of Mechanical Engineering  
Storrs, Connecticut 06269

**Xingwei Wang**

University of Massachusetts Lowell  
Department of Electrical and Computer  
Engineering  
Lowell, Massachusetts 01854  
E-mail: [xingwei\\_wang@uml.edu](mailto:xingwei_wang@uml.edu)

**Abstract.** Ultrasound generation from an optical fiber, based on the photoacoustic principle, is a promising approach to many ultrasonic applications, specifically those requiring wide bandwidth and compact size in order to achieve high resolution as well as the capability of being operated in limited space. A fiber-optic ultrasound generator using gold nanopores is reported. The gold nanopores, having high absorption efficiency, were fabricated using a focused ion beam (FIB) on the fiber endface, which was excited by a nanosecond laser in order to generate ultrasound signals via the photoacoustic principle. Experimental results demonstrate that these wide bandwidth ultrasound signals can be generated by this compact fiber-optic ultrasound generator fabricated using a FIB. © The Authors. Published by SPIE under a Creative Commons Attribution 3.0 Unported License. Distribution or reproduction of this work in whole or in part requires full attribution of the original publication, including its DOI. [DOI: [10.1117/1.OE.52.6.065005](https://doi.org/10.1117/1.OE.52.6.065005)]

Subject terms: photoacoustic; focused ion beam; ultrasound generator; fiber optic; gold nanopore.

Paper 130488P received Mar. 31, 2013; revised manuscript received May 13, 2013; accepted for publication May 24, 2013; published online Jun. 20, 2013.

## 1 Introduction

Ultrasound transducers are widely used in most ultrasound nondestructive testing and medical ultrasound imaging applications.<sup>1,2</sup> High-frequency (>30 MHz) and high-resolution (<100  $\mu\text{m}$ ) ultrasound transducers have become increasingly demanded in most advanced applications including dermatology,<sup>3</sup> ophthalmology,<sup>4</sup> intravascular imaging,<sup>5</sup> tomography,<sup>6</sup> and small animal imaging.<sup>7</sup> They are also valuable imaging tools for noninvasive studies of disease progression and regression.<sup>8,9</sup> With the conventional approach, which relies on a piezoelectric transducer, it is difficult to exceed a frequency of 20 MHz, and to minimize to a micron scale size for high spatial resolution.<sup>10</sup>

An attractive alternative to a traditional piezoelectric ultrasound transducer is an all-optical ultrasound transducer with both optical ultrasound generation and detection.<sup>11</sup> A photoacoustic ultrasound transducer provides significant advantages over a conventional piezoelectric one including a wide bandwidth and compact dimension. The optical ultrasound generator converts pulsed laser energy, exerted on the photoabsorptive layers, into thermoelastic waves.<sup>12</sup> The center frequency and bandwidth of the generated ultrasound is determined by the incident laser pulse.<sup>13</sup> One benefit of the ultra-fast laser technology is that laser pulses with short pulse widths can yield wide bandwidths of the ultrasound above 50 MHz.<sup>14</sup> In addition, the size and spacing of each generation element, which is defined by the focal spot of a laser beam, can be easily reduced to several microns.<sup>15</sup> The spatial resolution enhancement could be significantly

achieved by applying the photoacoustic technique on an optical fiber, typically with a diameter of 125  $\mu\text{m}$ .<sup>16</sup> Furthermore, an all-optical operation circumvents the need for electrical connections which cause the problem of electromagnetic interference. These unique features make the fiber-optic ultrasound transducers suitable for various advanced ultrasound applications.

However, the critical problem of the photoacoustic ultrasound generator is the relatively low amplitudes of the generated ultrasound signals, which result from a limit to the maximum laser power density in order to avoid damage to the photoabsorptive material. The photoacoustic energy conversion efficiency can be enhanced by increasing the optical absorption coefficient of the photoabsorptive material.<sup>17</sup> It has also been experimentally explored that some gold nanostructures are good absorption materials due to their high optical energy absorption capability at the plasmon resonant frequency.<sup>18–20</sup> Compared to random gold nanostructures, periodic gold nanostructures have higher absorption efficiency due to increased interaction time by localized surface plasmon.<sup>21</sup> Moreover, the thickness of the absorption material may affect the bandwidth as well. As the ultrasound propagates along the material, high frequency components attenuate faster than low frequency components. Therefore, a thin layer of gold nanostructure with periodic pattern is preferred. Furthermore, most of the photoacoustic ultrasound generators reported in the literature were bulky on substrates. With our work, we made an effort to miniaturize the device into  $\sim 100 \mu\text{m}$ ,

which is possible for the ultrasonic imaging applications in a restricted space.

For the fabrication of periodic gold nanostructures upon the optical fiber endface, a number of traditional micro/nano-fabrication tools have been brought to bear on the challenges. Submicron gold structures can be fabricated using femtosecond laser direct writing.<sup>22,23</sup> However, these methods have limitations such as limited precision and product geometry. Some delicate structures on fibers are constructed using micro-electro-mechanical systems.<sup>24–26</sup> However, they require a mask and the resolution is on a micrometer scale. Nanoimprint enhances the geometric accuracy and overall quick productivity in a nanometer scale, however, the pattern mold cannot be conveniently applied to the fiber endface.<sup>27</sup> Besides these techniques, the self-assembling technique is an exceptional method of bonding metal nanoparticles to fibers. However, it also has disadvantages including low concentration and random distribution which constrain the three-dimensional nanoscale fabrication upon the fiber endface.<sup>28</sup> The focused ion beam (FIB) can be used for this work because of its distinctive advantages such as high flexibility direct writing, ultra-precision processing, room temperature conditions, and no post-processing.<sup>29</sup>

In this paper, a fiber-optic photoacoustic ultrasound generator that has wide bandwidth and miniature size using gold nanopores was achieved. The FIB was used to mill the gold nanostructures directly on the fiber endface. The procedure used to mill high-quality and high-precision nanostructures on fiber at the nanometer scale was examined to illustrate the versatility and advantages of the FIB techniques for this application. Some fiber samples with the fabricated gold nanopores were used to demonstrate the photoacoustic ultrasound generation. It is proved that ultrasound signals can be generated by this approach and that the fiber-optic ultrasound generator can potentially be used in advanced ultrasonic applications.

## 2 Fabrication

### 2.1 Fiber Preparation

Single-mode fibers (SMF) with core/cladding diameters of 8/125  $\mu\text{m}$  and multimode fibers (MMF) with core/cladding diameters of 62.5/125  $\mu\text{m}$  were used. The protective coating was removed from a 1-mm long section after the fiber tip was cleaved. The cleaved angle of the fiber endface was controlled to an accuracy of 0.5 deg as measured by a fusion splicer (Fitel S177A). A gold layer with a thickness of 60 nm was sputter-coated onto the fiber endface. This gold layer served several purposes. First, it protected the fiber surface and prevented charging of the insulated fiber material. In effect, the quality of scanning electron microscope (SEM) imaging and FIB milling was increased. Second, after FIB patterning of the gold layer, the remaining gold sub-wavelength apertures or rods on the fiber endface were directly used as the functional material of the fiber-optic ultrasound generator. The objective gold nanopores on an optical fiber are shown in Fig. 1 with both top view and side view. The fiber tip was placed steadily upon the FIB stage using a conductive tape. The fiber pigtail was wound and pasted for further splicing and testing. The FIB stage was adjusted such that the FIB beam faced the fiber endface vertically.

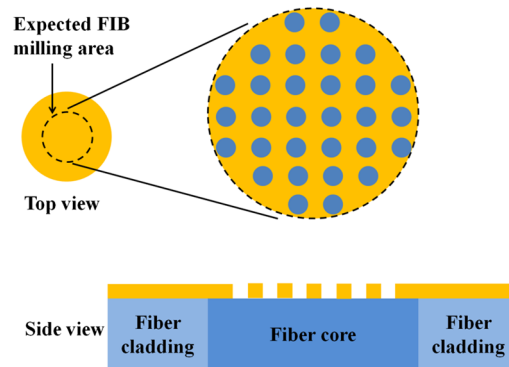


**Fig. 1** Schematic diagram of the objective gold nanopores on the fiber endface.

### 2.2 FIB Conditions

A computer-controlled dual-beam FIB instrument (FIB-SEM, Auriga series, Carl Zeiss, Oberkochen, Germany) was employed to create different gold nanopores on the fiber. The instrument used a combination of SEM and FIB with two focused beams on the coincidence point. In addition to providing SEM imaging, this instrument can rapidly mill materials via ion sputtering. Before fabrication, most of the patterning conditions need to be optimized specifically to the fiber sample. Accurate pattern shaping is unachievable at high energies due to large protrusions and nanopores formations; however, it can be obtained with low energy ions. Therefore, in order to significantly decrease the amount of redeposition, the gallium ion energy was set at 30 keV or lower if necessary. If a superior resolution is required it would be preferable to use a protective layer with the sample. In this case, the fiber endface was initially coated with a gold layer with a thickness of 60 nm to improve conductivity. Ion scattering from walls is another critical factor to the large feature depth. In this case, most of the nanostructures were shallow, so the scattering could be neglected.

For operation of the FIB, factors including the focus, astigmatism, and proper magnification of the particular ion beam aperture must be controlled to obtain high-quality nanostructures. Other important parameters to be adjusted include dwell time, beam current, scanning strategy, and the number of passes. Dwell time refers to the time interval that the beam spends on a single milling spot, and is set according to the milling rate and the expected milling depth. Note that the beam spot diameter is a theoretically calculated value based on a Gaussian distribution and depends on the beam current. Therefore, it should be properly selected according to the nanopore feature size. Line scanning is typically used for rectangular shapes whereas spiral scanning is typically used for circular shapes. The number of passes for each scanned pattern is also critical to milling rate and sidewall slope. In this case, the beam diameter was controlled between 3 and 300 nm by varying beam current 1 pA and 4 nA at a consistent incidence angle of 0 deg. Although FIB image could also be used to measure the feature dimension, this imaging mode damages the completed pattern severely. The SEM mode was used to monitor the FIB created surface features *in situ* with a 54-deg angle, and to measure the feature size with angle compensation.

### 2.3 Gold Nanopores

The key to the FIB milling technology is to operate FIB with the proper beam size, current, and energy used to remove a required amount of material from a pre-defined location and obtain high-precision structures in a controllable manner. In order to ensure the milling efficiency, the beam energy transferred from the ions to the target substrate should be sufficiently high. In order to ensure the milling accuracy, milling strategy such as a number of passes is important to prevent severe redeposition. For different samples and feature sizes, we need to select a proper beam current to balance the fabrication accuracy and the yield. For this case, to achieve a feature size of  $\sim 100$  nm, beam currents less than 10 pA was used to ensure the fabrication accuracy. Since the theoretical beam probe size of 10 pA about 13 nm is much smaller than the objective feature size of  $\sim 100$  nm, it is still potentially advantageous to further increase the beam current for higher throughput. The objective nanopores were fabricated by FIB milling nanopore array. After the removal of the gold material within the pore areas, the remaining gold materials form the gold nanopore array as shown in Fig. 2. Figure 2(a) shows gold nanostructure on the core area of a fiber endface. As shown in the embedded Fig. 2(b), FIB is flexible to align, mark, and fabricate various nanostructures on the fiber endface. In the zoom-in Fig. 2(c), the gold nanopores are 80 nm in diameter and 130 nm in spacing.

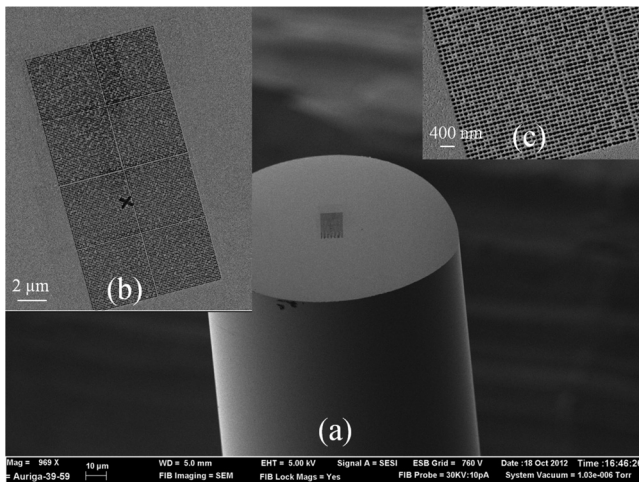


**Fig. 2** (a) Gold nanostructure on the core area of the fiber endface; (b) zoom-in FIB alignment mark and nanopores on the fiber endface; and (c) gold nanopores with 80 nm in diameter.

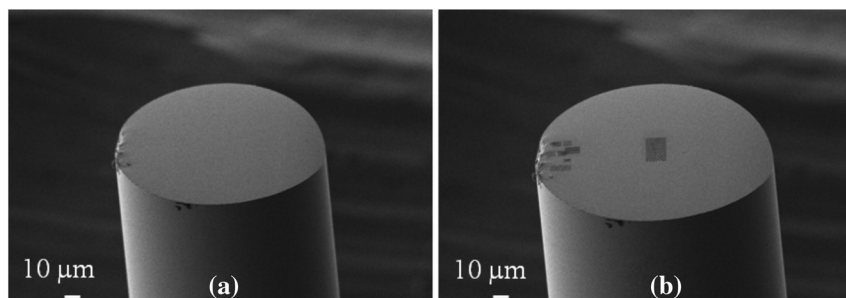


**Fig. 3** (a) Gold coated SMF before fabrication and (b) gold coated SMF after fabrication.

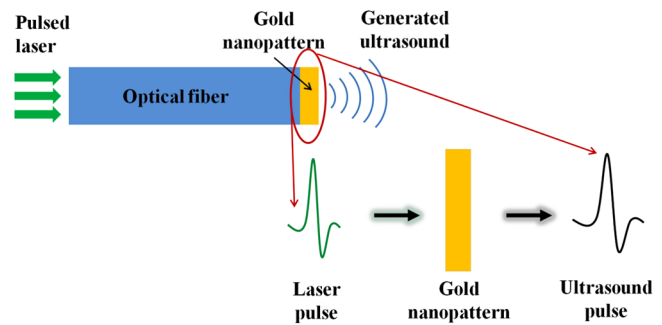


**Fig. 4** Schematic diagram of the photoacoustic principle.

Since only the fiber core area works for the photoacoustic ultrasound generation, only the core area was milled with the desired gold nanopores. Figure 3(a) and 3(b) shows the overview of the SMF before and after fabrication, respectively. Total milling time was about 30 min when a beam current of 10 pA was used.

## 3 Experiments

### 3.1 Photoacoustic Principle

As shown in Fig. 4, the fiber-optic photoacoustic generator is an optical fiber endface coated with the FIB-milled gold nanopores. When laser pulses are coupled into the fiber and guided to the gold nanopores, a portion of the optical irradiation energy is converted into thermal energy in the gold nanopores due to the high absorption efficiency. Then, due to the thermal effect, mechanical vibrations result from thermal expansion. Finally, ultrasound is excited and propagates in the adjacent medium. The advantage of this method is that the ultrasound pulse profile can be tailored by the laser pulse profile. This means broad bandwidth ultrasound can be generated by ultrashort laser pulses.

### 3.2 Experimental Setup

After FIB patterning of the gold layer on the fiber endface, the fiber sample was spliced with a fiber coupler (F810SMA-543, Thorlabs, Newton, New Jersey) to a nanosecond laser. Related experiments were performed in order to evaluate the photoacoustic generation efficiency through the gold nanopores. The schematic diagram of the experimental setup is shown in Fig. 5. A 532 nm Nd:YAG nanosecond laser (Surelite series, Continuum, Santa Clara, California) with a pulse duration of 5 ns and a repetition rate of 10 Hz was

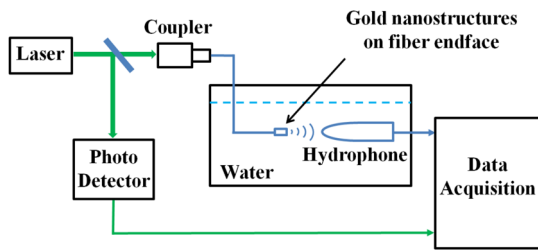


Fig. 5 Schematic diagram of the experimental setup.

used as the optical radiation source. The laser beam was split into two beams by a beam splitter. One of the beams was input into a photodetector (PDA10CS, Thorlabs) as a reference signal and another beam was coupled into the fiber pattern through the coupler. The gold nanopores were located directly on the fiber endface core area. The laser pulse was excited on the nanocomposite through the optical fiber. A hydrophone (HGL-0200, Onda, Sunnyvale, California) was placed about 1 to 2 mm away under water to collect the acoustic signals. The reference signals and the acoustic signals were transmitted to a data acquisition system (M2i.4032, Spectrum, Grosshansdorf, Germany) with a sampling rate of 50 MHz.

Figure 6(a) shows a photograph of the overall experimental setup. Translation stages were used to control the distance between the fiber tip and the hydrophone. Figure 6(b) shows an enlarged photograph of the miniature fiber-optic ultrasound generator with gold nanopores on it. Compared to the piezoelectric hydrophone, the fiber-optic ultrasound generator is much smaller, with a diameter of about 125  $\mu\text{m}$ .

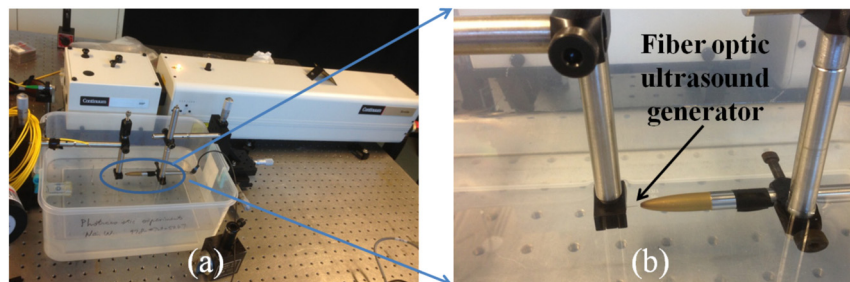


Fig. 6 (a) Photograph of the overall experimental setup and (b) enlarged photograph of the miniature fiber-optic ultrasound generator with gold nanopores on it.

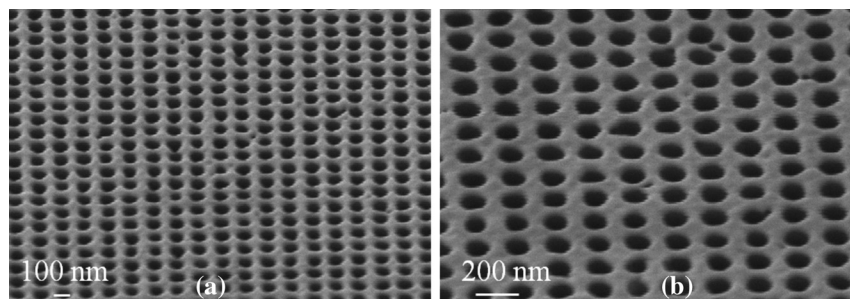
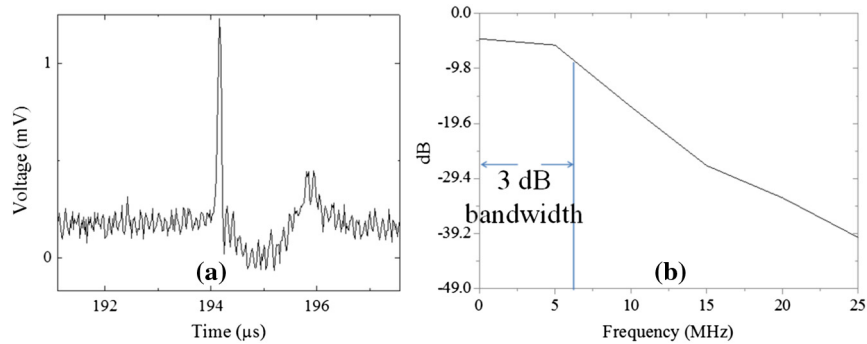


Fig. 7 The tested gold nanopores were 60 nm in thickness, 200 nm in spacing, and 80 nm in diameter on the MMF endface (a) at magnification of 104 kx; (b) at magnification of 135 kx.

## 4 Results and Discussions

Three parameters of the gold nanopores including thickness, spacing, and diameter affect the optical absorption efficiency. A larger thickness or smaller diameter leads to a narrower resonant peak and a rather uniform decrease in the absorption intensity. The absorption peak shifts to longer wavelength by increasing the spacing.<sup>30</sup> The tested gold nanopores located on the MMF endface were 60 nm in thickness, 200 nm in spacing, and 80 nm in diameter, so that the absorption peak was close to the excitation laser wavelength. The thickness could be controlled well by using a sputter coating process. During the FIB milling process, the ion beam focused on the nanopore areas, whereas the thickness of the rest of the gold area was kept the same as the coating thickness. The spacing of 200 nm and diameter of 80 nm were precisely fabricated by FIB. Figure 7 shows the SEM images of the gold nanopores in a different magnification. The flaws of the periodic pattern were caused by the fluctuation of the gold layer deposited on the fiber endface.

Figure 8(a) shows the ultrasound pulse that was generated from the fiber-optic ultrasound generator with the gold nanopores as shown in Fig. 7. The distance between the hydrophone and the fiber tip was about 1.5 mm. The excited optical pulse energy was about 3  $\mu\text{J}$  and the amplitude of the generated ultrasound signal was 2.73 kPa. The energy conversion efficiency can be improved by using other gold nanopatterns with different features, such as shape, size, spacing, and layer number, which possess higher optical energy absorption. A 3 dB bandwidth was 7 MHz as shown in Fig. 8(b). The bandwidth can be improved by using a shorter laser pulse.



**Fig. 8** (a) The profile of a typical generated ultrasound signal. (b) The frequency domain of the generated ultrasound signal showing the 3 dB bandwidth of approximately 7 MHz.

## 5 Conclusions

This paper reports a fiber-optic ultrasound generator having a wide bandwidth and miniature size and that uses gold nanopores. The gold nanopores were fabricated by milling periodic gold nanopores directly onto the optical fiber endface using FIB. The experimental results showed that an ultrasound signal with amplitude of 2.73 kPa and a 3-dB bandwidth of 7 MHz could be generated by the fiber-optic ultrasound generator. It proved that ultrasound signals could be generated by this miniature fiber-optic device which could be used in the advanced ultrasonic applications.

## Acknowledgments

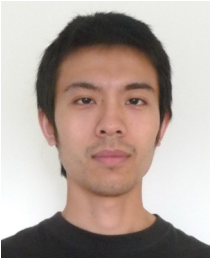
The authors would like to thank the funding support from National Science Foundation (CMMI: 1055358 CAREER, IIS 1208499, and MRI-R2: 0960022). The authors also appreciate Mr. Christopher Santeufemio at the Campus Materials Characterization Laboratory (CMCL) in the University of Massachusetts Lowell (UML) for his technical support of using FIB.

## References

- G. Sposito et al., "A review of non-destructive techniques for the detection of creep damage in power plant steels," *NDT&E Int.* **43**(7), 555–567 (2010).
- A. Baerwald et al., "Use of ultrasound biomicroscopy to image human ovaries *in vitro*," *Ultrasound Obstet. Gynecol.* **34**(2), 201–207 (2009).
- M. Vogt et al., "High frequency ultrasound for high resolution skin imaging," *Frequenz* **55**(1–2), 12–20 (2001).
- C. J. Pavlin and F. S. Foster, "Ultrasound Biomicroscopy of the Eye," Springer-Verlag, New York (1994).
- B.-Y. Hsieh et al., "Integrated intravascular ultrasound and photoacoustic imaging scan head," *Opt. Lett.* **35**(17), 2892–2894 (2010).
- C. Li and L. V. Wang, "Photoacoustic tomography and sensing in biomedicine," *Phys. Med. Biol.* **54**(19), R59–R97 (2009).
- D. H. Turnbull, "In utero ultrasound backscatter microscopy of early stage mouse embryos," *Comput. Med. Imaging Graph.* **23**(1), 25–31 (1999).
- D. H. Turnbull et al., "Ultrasound backscatter microscope analysis of mouse melanoma progression," *Ultrasound Med. Biol.* **22**(7), 845–853 (1996).
- D. E. Goertz et al., "High-frequency doppler ultrasound monitors the effects of antivasular therapy on tumor blood flow," *Cancer Res.* **62**(22), 6371–6375 (2002).
- S. Ashkenazi et al., "Optoacoustic imaging using thin polymer étalon," *Appl. Phys. Lett.* **86**(13), 134102 (2005).
- N. Wu et al., "Study of the compact fiber optic photoacoustic ultrasonic transducer," *Proc. SPIE* **8345**, 83453Z (2012).
- N. Wu et al., "High-efficiency optical ultrasound generation using one-pot synthesized polydimethylsiloxane-gold nanoparticle nanocomposite," *J. Opt. Soc. Am. B* **29**(8), 2016–2020 (2012).
- N. Wu et al., "Theoretical analysis of a novel ultrasound generator on an optical fiber tip," *Proc. SPIE* **7677**, 76770X (2010).
- Y. Hou et al., "Optical generation of high frequency ultrasound using two-dimensional gold nanostructure," *Appl. Phys. Lett.* **89**(9), 093901–093903 (2006).
- S.-W. Huang et al., "High-resolution ultrasonic imaging using an étalon detector array," *Appl. Phys. Lett.* **93**(11), 113501–113503 (2008).
- E. Biagi et al., "Fiber optic broadband ultrasonic probe," in *2008 IEEE Sensors, SENSORS 2008*, Lecce, Italy, pp. 363–366, Institute of Electrical and Electronics Engineers Inc., Piscataway, NJ (2008).
- S. J. Davies et al., "Laser-generated ultrasound: its properties, mechanisms and multifarious applications," *J. Phys. D: Appl. Phys.* **26**(3), 329–348 (1993).
- Y. Tian et al., "Numerical simulation of fiber-optic photoacoustic generator using nanocomposite materials," *J. Comput. Acoust.* **21**(2), 1350002 (2013).
- X. Yang et al., "Nanoparticles for photoacoustic imaging," *Wiley Interdiscip. Rev. Nanomed. Nanobiotechnol.* **1**(4), 360–368 (2009).
- N. Wu, K. Sun, and X. Wang, "Fiber optics photoacoustic generation using gold nanoparticles as target," *Proc. SPIE* **7981**, 798118 (2011).
- T. L. Temple and D. M. Bagnall, "Optical properties of gold and aluminium nanoparticles for silicon solar cell applications," *J. Appl. Phys.* **109**(8), 084343 (2011).
- X. Ma et al., "Surface-enhanced Raman scattering sensor on an optical fiber probe fabricated with a femtosecond laser," *Sensors* **10**(12), 11064–11071 (2010).
- K. Venkatakrishnan et al., "Femtosecond pulsed laser direct writing system," *Opt. Eng.* **41**(6), 1441–1445 (2002).
- A. Petrušis et al., "The align-and-shine technique for series production of photolithography patterns on optical fibres," *J. Micromech. Microeng.* **19**(4), 047001 (2009).
- S. Feng et al., "Fiber coupled waveguide grating structures," *Appl. Phys. Lett.* **96**(13), 133101 (2010).
- C. Liberale et al., "Micro-optics fabrication on top of optical fibers using two-photon lithography," *IEEE Photon. Technol. Lett.* **22**(7), 474–476 (2010).
- G. Kostovski et al., "Nanoimprinted optical fibres: biotemplated nanostructures for SERS sensing," *Biosens. Bioelectron.* **24**(5), 1531–1535 (2009).
- G. F. S. Andrade, M. Fan, and A. G. Brolo, "Multilayer silver nanoparticles-modified optical fiber tip for high performance SERS remote sensing," *Biosens. Bioelectron.* **25**(10), 2270–2275 (2010).
- S. H. Ahn, D. M. Chun, and C. S. Kim, "Nanoscale hybrid manufacturing process by nano particle deposition system (NPDS) and focused ion beam (FIB)," *CIRP Ann. Manuf. Technol.* **60**(1), 583–586 (2011).
- H. Hguyen et al., "Modeling of gold circular sub-wavelength apertures on a fiber endface for refractive index sensing," *Photon. Sens.* **2**(3), 271–276 (2012).



**Ye Tian** received his MS degree from the Institute of Modern Optics, Nankai University, Tianjin, China, in 2008. He earned his BS degree in communication engineering from Nankai University, Tianjin, China, in 2005. He is currently pursuing the PhD degree at the Department of Electrical and Computer Engineering, University of Massachusetts Lowell, Lowell, MA, USA. His current research interests include biosensors, fiber optic sensors, micro-electro-mechanical systems (MEMS), and FIB.



**Nan Wu** received a PhD degree from the Department of Electrical and Computer Engineering, University of Massachusetts (UMass) Lowell, Lowell, MA, USA, in 2012. He is currently a post-doctoral researcher with UMass. His current research interests include fiber optic pressure sensors, fiber optic photoacoustic generators, and photoacoustic imaging.



**Xiaotian Zou** received an MS degree in mechanical engineering from the University of Connecticut, Storrs-Mansfield, CT, USA, in 2010. He is currently pursuing the PhD degree with the Department of Biomedical Engineering and Biotechnology, University of Massachusetts Lowell, Lowell, MA, USA. His current research interests include control and data analysis algorithms for bio-systems and optical biosensors.



**Haitham Felemban** graduated from Northern Illinois University with a bachelor's degree in mechanical engineering in May 2012. He is pursuing his master's degree in mechanical engineering from the University of Connecticut with an emphasis in dynamics and control.



**Chengyu Cao** has been an assistant professor in the Mechanical Engineering Department at the University of Connecticut since 2008. Prior to that, he was a research scientist in the Department of Aerospace and Ocean Engineering at the Virginia Polytechnic Institute and State University. He received his PhD in mechanical engineering from the Massachusetts Institute of Technology in 2004. He earned his BS degree in electronics and information engineering from Xi'an Jiaotong University, China and MS in manufacturing engineering from Boston University in 1995 and 1999, respectively. His research is in the area of dynamics and control, unmanned systems, and mechatronics.



**Xingwei Wang** is an associate professor in the Department of Electrical and Computer Engineering, University of Massachusetts Lowell, Lowell, MA, USA. Her current research interests include optical sensors for medical, chemical and industrial applications, assistive technology program, nanoprobe design and fabrication, self-assembled nanostructures, optical biosensing and biomedical devices, optical imaging, and MEMS technology and electromagnetic wave propagation.